Mean square radii of nuclei calculated with the Woods-Saxon potential

Z. Łojewski, B. Nerlo-Pomorska, and K. Pomorski
Institute of Physics, M. Curie-Skłodowska University, PL-20031 Lublin, Poland

J. Dudek
University Louis Pasteur, Theoretical Physics Division, F-67037 Strasbourg CEDEX, France
(Received 31 May 1994)

The realistic single-particle Woods-Saxon potential was used to evaluate the mean-square charge radii of even-even nuclei. The results are compared with experimental data and theoretical values obtained with the single-particle Nilsson potential. An evidence for a need of improving of the "universal" parametrization of the deformed Woods-Saxon Hamiltonian, suggested earlier, is investigated in more detail and a possible solution of the optimization problem is formulated.

PACS number(s): 21.10.−k

I. INTRODUCTION

A compilation of the all experimental mean-square charge radii $\langle r^2 \rangle$, obtained from elastic electron scattering on nuclei is presented in [1]. The use of laser and mass spectroscopy techniques in measurements of the isotopic shifts in the nuclear mean-square charge radii (MSR) has resulted in a wealth of new information concerning this fundamental property of nuclei [2–5]. The systematics of the MSR and quadrupole moments can be used to test the quality of theoretical models, and in particular a competition between the macroscopic, "liquid-drop" features and shell closures determining the sizes and shapes of nuclei.

Over the years a number of theoretical papers have been devoted to calculations of the isotopic shifts in the MSR of the nuclei. For instance, in Refs. [6,7], the ground-state static electric quadrupole and hexadecapole moments and MSR of even nuclei were calculated microscopically using the standard Nilsson single-particle potential.

The later papers [8–10] on the MSR have been based on the microscopic collective dynamical model and the Nilsson potential with a set of parameters that are partially determined by the Hamiltonian itself [11]. More precisely, the Nl-shell-dependent Nilsson model parameters μ_{Nl} and κ_{Nl} have been re-defined using three constants adjusted simultaneously for the protons and neutrons while the Nl dependence in μ and κ has been defined phenomenologically using the corresponding nucleonic wave functions. The quality of the new parametrization has been tested on the spectrum of the spherical nuclei only. However, it was shown [6–10] that within parametrization [11] it was possible to reproduce the experimental isotopic shifts of the MSR. The theoretical shifts were too large on average. Moreover, it has been shown in Ref. [12] that the isotopic shifts of the mean-square radii are well reproduced when the isotopic factor in the oscillator frequency $\hbar\overset{o}{\omega}_0$ in the Nilsson potential was omitted.

The choice of the single-particle nuclear potential is of fundamental importance for a wide variety of nuclear calculations. The aim of the present investigation is the analysis of the mean-square radii of nuclei calculated with the realistic Woods-Saxon potential [13].

An axially symmetric Woods-Saxon (WS) potential has been earlier applied in predicting and explaining the structure of the high-spin isomers [14], in analyzing the nucleon binding energies [15], in reproducing the static nuclear equilibrium deformations and moments [16], in calculating the fission barriers and the number of the single-particle effects for strongly deformed and fast rotating nuclei [17,18]. It is of interest to check if the theoretical predictions of the mean-square radii calculated with the Woods-Saxon potential reproduce the experimental data, especially for nuclei far from the β stability line.

An important advantage of the so-called universal parametrizations of nuclear average-field Hamiltonian, i.e., those which employ one single set of constants for a very large number of nuclei (e.g., for all nuclei with $Z > 20$ and $N > 20$) is that they may be used for extrapolating some nuclear properties into yet unknown nuclear regions.

A universal set of parameters (cf. [13] for references) adopted to the Woods-Saxon Hamiltonian has been based on the earlier Rost [19] parametrization of the central nuclear potential; however the spin-orbit part of the potential which is mainly responsible for the single-particle level order has been reanalyzed using a rich body of experimental data in particular for the deformed nuclei.

While successful in describing quite well, on the average, the single-particle level order at the nuclear equilibrium deformations in nuclei with $Z, N > 20$, the universal set of parameters [13] suffered from the unusually large radius parameters introduced originally by Rost.

The corresponding values of $r_{0,n} = 1.347$ fm and $r_{0,p} = 1.275$ fm for neutrons and protons, respectively, exceed markedly the radius-parameter values known from the literature of other nuclear phenomena. Moreover, the nuclear high-spin calculations have revealed that the microscopic results for the nuclear moments of inertia

can be markedly exaggerated as well if the above radius-parameters are used.

A series of tests of the idea of a universal parametrization of the nuclear Woods-Saxon average field has been made in Ref. [20] where $B(E2)$ and the nuclear separation energies have been calculated and compared with the experimental data for several hundreds of nuclei throughout the periodic table.

It has been concluded that the central potential radius parameters need to be decreased to about 1.25 fm for protons and neutrons in order to improve an average agreement with experiments on both quadrupole moments and on the average rotational properties of deformed nuclei.

It is the purpose of this study to determine in more detail the size of derivations caused by the above-mentioned deficiency of the central potential parametrization in order to suggest more precisely an amelioration of the overall performance of the Woods-Saxon Hamiltonian.

The microscopic static calculation of the MSR has been performed in two steps: calculations of the equilibrium deformations of nuclei and the evaluation of the MSR at the equilibrium. The calculations were performed for the nuclei around Sn with $46 \leq Z \leq 60$ and for the rare-earth nuclei $60 \leq Z \leq 70$. The method of calculating the MSR is described in Sec. II. In Sec. III the main results are presented. Conclusions are drawn in Sec. IV.

II. THEORETICAL MODEL

The calculations were performed for even-even isotopes in the range of $46 \leq Z \leq 60$ and $Z \leq N \leq 120$, i.e., in the Sn and in the rare-earth region with $60 \leq Z \leq 70$ and $Z \leq N \leq 150$. The quadrupole β_2 and hexadecapole β_4 deformations were taken into account.

The ground-state energy of each nucleus has been evaluated using the Strutinsky [21] prescription. The energy of a nucleus consists of the macroscopic liquid drop $E_{\rm LD}$ [22] part and the shell correction $\delta E_{\rm shell}$ describing the shell and the pairing effects:

$$E_{\rm tot} = E_{\rm LD} + \delta E_{\rm shell}. \tag{1}$$

The shell corrections in Eq. (1) have been calculated as usual [21] employing a correction polynomial of the sixth order. We have used the single-particle spectra of the Woods-Saxon deformed potential. As this potential is widely described in the literature (see [13]), we restricted ourselves to a brief presentation of the basic formulas.

The Woods-Saxon potential consists of the central part $V_{\rm cent}$, the spin-orbit part $V_{\rm so}$, and the Coulomb potential $V_{\rm Coul}$ for protons:

$$V^{\rm WS}(\vec{r},\vec{p},\vec{s};\beta) = V_{\rm cent}(\vec{r};\beta) + V_{\rm so}(\vec{r},\vec{p},\vec{s};\beta) + V_{\rm Coul}(\vec{r};\beta) \tag{2a}$$

with

$$V_{\rm so}(\vec{r},\vec{p},\vec{s};\beta) = -\lambda(\nabla V_{\rm cent} \times \vec{p}) \cdot \vec{s}. \tag{2b}$$

The central part is defined by

$$V_{\rm cent}(\vec{r};\beta) = \frac{V_0[1 \pm \kappa(N-Z)/(N+Z)]}{[1+\exp(l(\vec{r};\beta)/a)]}, \tag{3}$$

where a is the diffuseness of the nuclear surface, the plus $(+)$ sign holding for protons, the minus $(-)$ sign for neutrons, and $\kappa = 0.86$ [13]. The set of β_λ parameters is denoted by β. The function $l(\vec{r},\beta)$, describing the distance between a given point $\vec{r}$ and the nuclear surface, has been determined numerically [13]. For spherical nuclei $l(\vec{r},\beta=0) = r - R_0$, where $R_0 = r_0 A^{1/3}$ is the radius of the corresponding spherical nucleus. In the above formulas β stands for the parameters characterizing the nuclear shape:

$$R(\theta) = c(\beta) R_0 \left[1 + \sum_\lambda \beta_\lambda Y_{\lambda 0}(\cos\theta)\right] . \tag{4}$$

The function $c(\beta)$ ensures the conservation of the nuclear volume with a change in the nuclear shape.

In our calculations we have used the single-particle WS potential with the "universal" variant of its parameters adjusted to the single-particle levels of all odd-A nuclei with $A \geq 40$. The values of the 12 constants which determine the WS potential parametrization are specified in Ref. [13].

The residual pairing interaction has been treated within the usual BCS procedure with the pairing strength parameters taken from Ref. [23]. The equilibrium deformation parameters $(\overset{o}{\beta}_2, \overset{o}{\beta}_4)$ have been calculated by minimizing the total nuclear energy according to Eq. (1).

The formulas for the microscopic multipole moments Q_λ, calculated as the mean values of the $\hat{Q}_\lambda$ operators in the ground-state BCS wave function, are given by

$$Q_\lambda = \sum_\nu q^\lambda_{\nu\nu} 2 v^2_\nu, \tag{5}$$

where $q^\lambda_{\nu\nu}$ denotes the diagonal matrix element of the $\hat{Q}_\lambda$ operator and v_ν denotes the BCS particle occupation factor in a single-particle state $|\,\nu\rangle$. The summation runs over proton states.

The proton mean-square radii $\langle r_p^2\rangle^A$ are related to the electric monopole moments Q_0 by

$$\langle r_p^2\rangle^A = Q_0/Z. \tag{6}$$

The charge distribution is obtained by the convolution of the ponctual density (stemming from sp wave functions) with a Gaussian form factor $f(\vec{r})$ of the proton:

$$f(\vec{r}) = \frac{1}{(\sigma\sqrt{\pi})^3} e^{-\vec{r}^2/\sigma^2}, \tag{7a}$$

where $\sigma = 0.65$ fm [24]. It is proven in [24] that the result of folding process on the mean-square charge radii $\langle r^2\rangle^A$ can be approximated by the following formula:

$$\langle r^2\rangle^A = \langle r_p^2\rangle^A + 1.5\sigma^2. \tag{7b}$$

The experimental mean-square charge radii obtained from electron scattering [1] and their isotopic shifts from

the laser techniques [2–5] allow us to determine the absolute values of the experimental RMS for a large number of isotopes. Our calculated radii $\langle r^2\rangle^A$ will be compared with this experimental information in the following section.

III. RESULTS

The equilibrium deformations were found by minimizing the ground state potential energies [see Eq. (1)] in the β_2-, β_4- deformation space. The two-dimensional grid of deformations,

$$\beta_2 \in [-0.40\ (0.05)\ 0.45], \tag{8a}$$

$$\beta_4 \in [-0.12\ (0.04)\ 0.12], \tag{8b}$$

has been presently used. The calculations of the equilibrium deformations have been carried out by using the "average" level spectrum of the ^{120}Xe nucleus for the nuclei in the Sn region ($Z \in [46\text{–}58]$) and ^{162}Dy for the rare-earth nuclei ($Z \in [60\text{–}70]$). Nevertheless in latter calculations of the RMS the proper spectrum for every nucleus was used.

The characteristic plot of the equilibrium deformations $(\overset{o}{\beta}_2, \overset{o}{\beta}_4)$ of the rare-earth nuclei is given in Fig. 1 for illustration. It can be seen from the figure that the position of the equilibrium moves from a spherical shape for the nuclei with N close to the magic number N=82, towards positive hexadecapole deformations for lighter rare-earth nuclei (Nd, Sm, Gd). The medium heavy nuclei have the maximum quadrupole deformation while β_4 is close to zero. The heavier rare-earth nuclei show the characteristic negative hexadecapole and decreasing quadrupole deformations.

In Fig. 2 the mean-square radii of Sn-region isotopes are shown. The results are presented for all the even-even combinations of $46 \le Z \le 58$ and $Z \le N \le 100$. The curves are labeled by the chemical symbols of the elements. The left-hand side scale corresponds to the lightest nucleus, palladium. The other curves are shifted upwards by 2 fm^2 each.

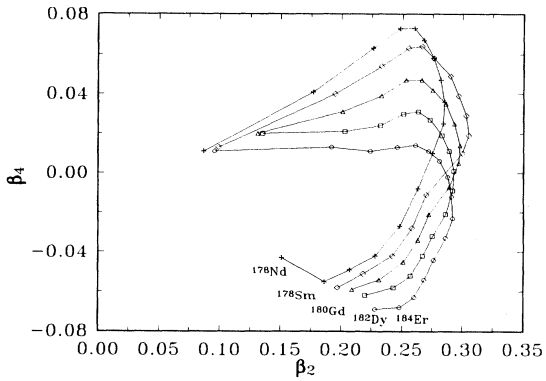

FIG. 1. Values of the equilibrium deformation parameters ($\overset{o}{\beta}_2$ and $\overset{o}{\beta}_4$) for rare-earth region of nuclei. The terminal values of mass number A and chemical symbols of elements are indicated at the end of each curve.

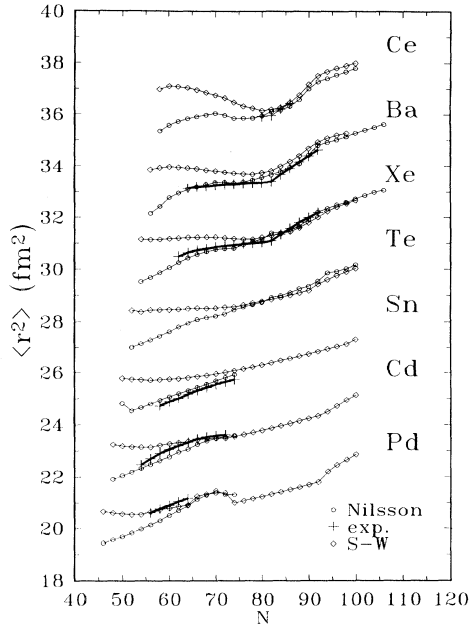

FIG. 2. The mean-square radii of nuclei $\langle r^2\rangle$ of the Sn region. The results obtained with the WS potential are denoted by empty diamonds, the Nilsson spectrum, as in Ref. [12], by circles, and experimental values by crosses. The left-hand scale corresponds to the palladium element. For clarity the results of the remaining nuclei are shifted upwards by 2 fm^2 each.

The MSR calculated with the single-particle Woods-Saxon potential are denoted by the empty diamonds. The results corresponding to the calculations with the Seo-Nilsson [11] single-particle spectrum and without isotopic factors in the oscillator frequency $\hbar\overset{o}{\omega}_0$ as in [12] are marked by empty circles. The crosses, joined by solid lines, denote the experimental values [1–5]. It is seen that the $\langle r^2\rangle$ calculated with the single-particle Nilsson potential reproduce the experimental data better.

The MSR obtained with the Woods-Saxon model are in general too big as compared to the experimental data. This effect is especially evident for the neutron-deficient isotopes, far from the β stability line. Also the dependence of $\langle r^2\rangle$ versus neutron numbers is not proper.

Figure 3 gives similar results for the rare-earth region ($Z \in 60\text{–}70$). As in Fig. 2 the left-hand scale corresponds to the lighter nucleus, neodymium. As previously, each next curve is shifted upwards by 2 fm^2. The results of MSR based on the WS potential are on average about 0.5–1.0 fm^2 larger than the experimental data. Unfortunately the experimental data for neutron-deficient isotopes of the tested nuclei do not exist for isotopes where the difference between results of Nilsson and WS single-particle spectrum becomes very large ($\sim$ 1.5–2.0 fm^2).

In order to explain the discrepancies between results of calculations of $\langle r^2\rangle$ with the WS potential and the experimental data, far from the β line of stability we have an-

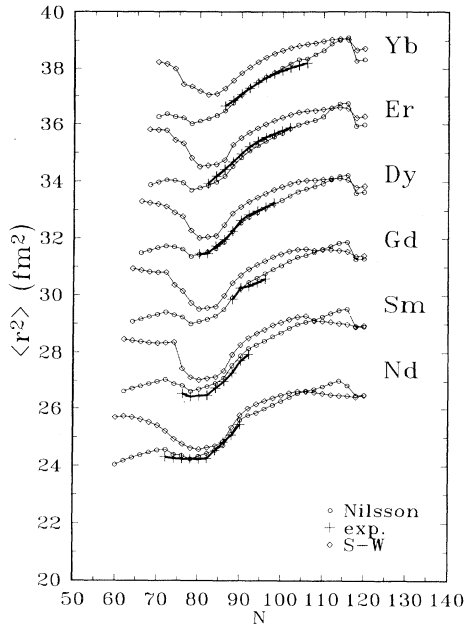

FIG. 3. The same as in Fig. 2, but for the rare-earth of nuclei. The left-hand scale corresponds to the neodymium isotopes.

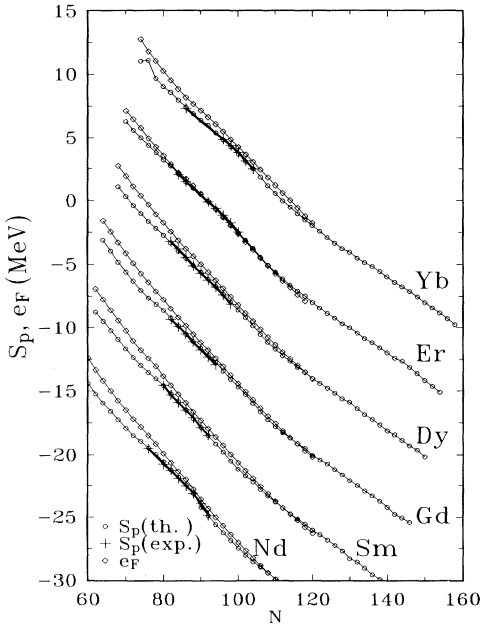

FIG. 4. The separation energies of proton S_p, defined as in Eq. (9) and Fermi levels e_F obtained with the WS potential for rare-earth of nuclei. The left-hand scale corresponds to the dysprosium isotopes. The results of the remaining nuclei are shifted upwards or downwards by 5 MeV each.

alyzed the proton and neutron separation energies. The results are presented in Figs. 4 and 5.

The separation energies (proton or neutron) are defined by

$$S_p(N,Z) = 0.5[B(N,Z) - B(N,Z-2)], \tag{9a}$$

$$S_n(N,Z) = 0.5[B(N,Z) - B(N-2,Z)], \tag{9b}$$

where $B(N,Z)$ denote the binding energy of even-even nuclei, with Z protons and N neutrons. They can be also interpreted as the experimental values of the actual Fermi levels.

In Figs. 4 and 5 the proton and neutron separation energies $S_{p,(n)}$ of rare-earth region nuclei are shown. The experimental values are denoted by crosses. The theoretical ones, obtained using formula (9a and 9b) and the nuclear masses from the tables by Möller and Nix [25], are shown by circles. The corresponding Fermi levels obtained with the WS potential are denoted by diamonds. The left-hand scale corresponds to the dysprosium isotopes. Results for other nuclei are shifted upwards or downwards by 5 MeV.

It is seen that for nuclei near the β stability line the experimental separation energy of the last nucleon is in a very good agreement with the actual value of the Fermi level. The opposite situation is for the neutron-deficient nuclei far from the β stability line. In this region the difference between the experimental $S_{p,(n)}$ values and the Fermi energies is about 2–3 MeV, occasionally 4 MeV. The calculations show that Fermi levels for protons lay too high (or the depth of the WS potential is too small) and exactly reverse for neutrons. It means that the universal set of parameters of the WS potential is good for nuclei near to the β stability line but for isotopes far

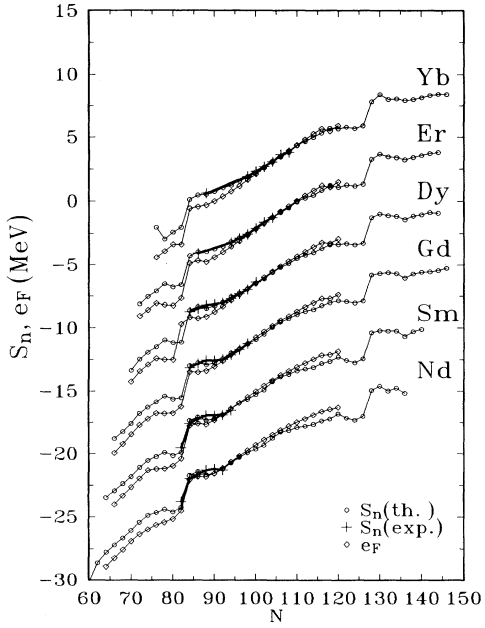

FIG. 5. The same as in Fig. 4 for neutrons.

from this line it does not reproduce the binding energies correctly.

The position of the Fermi level depends mainly on the radius parameter, r_0 and depth of the central potential, V. It is worth noticing that variation of r_0 and V act on the single-particle spectrum mainly by "pushing it up" or "pulling it down" whereas the other parameters of the potential are responsible mainly for the relative positions of levels.

The depth of the central potential is parametrized as

$$V = V_0[1 \mp \kappa(N - Z)/(N + Z)] \qquad (10)$$

with the plus sign (+) for protons and the minus (−) for neutrons. The universal set of parameters quoted in [13] employed too large values of the radius constants as indicated in Sec. I. Consequently, for a fixed potential depth the calculated Fermi levels should appear too low. This has been counteracted by adjusting the V_0 and κ constants in Eq. (10) to several nuclei close to β stability line.

Since the effective potential depth is determined by both V_0 and κ values it becomes clear that a large range of the N and Z variations will be necessary to determine V_0 and κ with a sufficiently high precision. Our analysis, although partly model dependent, has been extended to the neutron-deficient nuclei in which the variation of the isospin factor $(N - Z)/(N + Z)$ is relatively rapid. Consequently, our results should contain an improved information on the corresponding neutron deficient nuclei. While the isotopic dependence of the depth of the potential is controlled by two parameters, V_0 and κ, the Fermi energies are also strongly radius dependent. Our results on the MSR values confirm the earlier observation of too large radius constants contained in the universal set of [13]. At the same time they indicate that the isotopic spin dependence on Fermi energies is systematically too strong. Consequently, the modification (decrease) of the improved radius parametrization of the new universal set to be constructed should be accompanied by an increase of V_0 and a decrease of κ parameters.

IV. CONCLUSIONS

The following conclusion can be drawn from our investigation:

The model with the Woods-Saxon potential gives the RMS in good agreement with experimental data on the nuclei near the β stability line only. The WS values of RMS for the neutron deficient isotopes are too large.

The proton separation energies estimated with the Woods-Saxon potential are too large for the neutron-deficient isotopes, whereas for neutrons they are too small.

Since the universal set of the Woods-Saxon potential parameters has been fitted only for nuclei near the β stability line, their use in the present form to the neutron deficient region seems to be rather risky.

The calculations with Skyrme forces suggest that the isotopic dependence of the depth of the nuclear potential is weaker than that proposed in Woods-Saxon potential. The new list of parameters for the WS potential should therefore take into account the new information following from our study: (a) smaller values of the central potential radius parameter, (b) weaker isotopic spin dependence [smaller κ-values in Eq. (10)], (c) deeper central potential constant [larger V_0 in Eq. (10)].

The second of the above observations corresponds, in fact, with the results obtained by using different arguments in Ref. [26].

This work was supported partly by KBN, Project No. 2 P 302 05206.

[1] H. de Vries, C. W. de Jager, and C. de Vries, At. Data Nucl. Data Tables **36**, 495 (1987).
[2] E.W. Otten, in *Treatise on Heavy Ion Science*, edited by D. Allan Browley (Plenum, New York, 1984), Vol. 8, p. 517.
[3] P. Aufmuth, K. Heiling, and A. Steudel, At. Data Nucl. Data Tables **37**, 455 (1985).
[4] S. Raman, C.H. Malarkey, W.T. Milner, C.W. Nestor, Jr., and P.H. Stelson, At. Data Nucl. Data Tables **36**, 1 (1987).
[5] H. Mach *et al.*, Nucl. Phys. **A523**, 197 (1991).
[6] B. Nerlo-Pomorska, Nucl. Phys. **A259**, 481 (1976).
[7] P. Rozmej, Nucl. Phys. **A445**, 495 (1985).
[8] B. Nerlo-Pomorska and K. Pomorski, Ann. Univ. MCS, Sec. AAA, **XLIII/XLIV**, 211 (1988/1989).
[9] B. Nerlo-Pomorska, K. Pomorski, and B. Skorupska, in Proceedings of XXI Masurian School on Nuclear Phys. 1990 (unpublished).
[10] B. Nerlo-Pomorska and B. Skorupska, Ann. Univ. MCS, Sect. AAA, **XLV**, 90 (1990).
[11] T. Seo, Z. Phys. A **324**, 43 (1986).
[12] B. Nerlo-Pomorska, K. Pomorski, and B. Skorupska-Mach, Nucl. Phys. **A562**, 180 (1993).
[13] S. Ćwiok, J. Dudek, W. Nazarewicz, J. Skalski, and T. Werner, Comput. Phys. Commun. **46**, 379 (1987).
[14] J. Dudek, Z. Szymański, T. Werner, A. Faessler, and C. Lima, Phys. Rev. C **26**, 1772 (1982).
[15] J. Dudek, Acta Phys. Pol. B **9**, 919 (1978).
[16] G. Leander, W. Nazarewicz, G. Bertch, and J. Dudek, Nucl. Phys. **A453**, 58 (1986).
[17] J. Dudek, W. Nazarewicz, and A. Faessler, Nucl. Phys. **A412**, 61 (1984).
[18] W. Nazarewicz, J. Dudek, R. Bengtsson, T. Bengtsson, and I. Ragnarsson, Nucl. Phys. **A435**, 397 (1985).
[19] E. Rost, Phys. Lett. **26B**, 184 (1968).
[20] S. Kahane, S. Raman, and J. Dudek, Phys. Rev. C **40**, 228 (1989).
[21] V.M. Strutinsky, Nucl. Phys. **A95**, 420 (1967); **A122**, 1 (1968).
[22] V. Myers and W.J. Swiatecki, Ark. Fys. **36**, 343 (1967).
[23] J. Dudek, A. Majhofer, and J. Skalski, J. Phys. G **6**, 447 (1980).
[24] P. Quentin, in Proceedings of the International Conference on Nuclear Self-Consistent Fields, Trieste, 1975, p. 297 (unpublished).
[25] P. Möller, J. R. Nix, W. D. Myers, and W. J. Swiatecki, At. Data Nucl. Data Tables (to be published).
[26] R.D. Amado, Bin Shao, and N.R. Walet, Phys. Lett. B **314**, 159 (1993).